

Entanglement-Assisted Coherent Control in Nonreactive Diatom-Diatom Scattering

Jiangbin Gong, Moshe Shapiro *, and Paul Brumer
*Chemical Physics Theory Group,
Department of Chemistry,
University of Toronto
Toronto, Canada M5S 3H6*
(Dated: September 15, 2018)

Intriguing quantum effects that result from entangled molecular rovibrational states are shown to provide a novel means for controlling both differential and total collision cross sections in identical particle diatom-diatom scattering. Computational results on elastic and inelastic scattering of para-H₂ and para-H₂ are presented, with the collision energy ranging from 400 cm⁻¹ to the ultracold regime. The experimental realization and possible extension to other systems are discussed.

I. INTRODUCTION

Recent years have witnessed an increasing interest in controlling molecular and atomic processes [1, 2, 3]. The central principle of Coherent Control (CC) teaches that such control can be achieved by using coherent laser fields to induce constructive or destructive interference between multiple indistinguishable pathways to the same final state. The yield of desired or undesired product can thus be enhanced or suppressed by manipulating the resultant quantum interference terms. Thus far, most experimental and theoretical studies of CC of atomic and molecular processes have focused on unimolecular reactions or half collisions, such as photodissociation, photoionization and photoassociation.

By contrast, controlling full collision processes such as atom-atom scattering, atom-molecule scattering, and molecule-molecule scattering remains a significant challenge. Existent studies along this direction have largely employed a number of approaches [4, 5, 6, 7, 8]. The first [4, 5, 6] actively manipulates coherent light sources to alter the interaction potential of the colliding particles. For example, in ultracold atom-atom collisions, the scattering cross sections can be extensively modified by using laser fields that are in near resonance with one of the excited molecular electronic states [4, 5], or by employing a d.c. field that induces an additional dipole-dipole interaction potential [6]. However, it appears difficult to use this approach to control atom-molecule or molecule-molecule scattering, since the number of degrees of freedom is much larger than that in atom-atom scattering. A second approach is laser catalysis [8] in which the laser field photons serve as a catalyst. In this case the laser accelerates (or suppresses) the reaction by inducing a barrier hopping process, via a virtual excitation to a bound excited state, while remaining unchanged at the end of the event. The third approach, which is the subject of this study, is coherent control [7]. Although the general theory of collisional CC has been worked out [7] and conditions for control established [9] the experimental problem remains as to how one can introduce the required adjustable quantum phases and amplitudes into coherent scattering processes in a fashion so as to introduce control based upon quantum interference. That is, several recent studies on CC of collisions in model scattering systems [9] make clear that, for collisions of non-identical molecules, coherent control requires that one establish subtle quantum correlations between the translational and internal degrees of freedom of the reactants. Setting up the required initial states presents an experimental challenge, since it requires coherent matter-wave beams in which the internal states of the molecule are correlated in a precise way with the translational states.

Such correlated translational-internal states are not required, however, if one attempts coherent control in the collision of identical molecules, i.e., AB + AB. Rather, it suffices [10] to prepare the reactants in superpositions of initial rovibrational states. In this case, in accord with Ref. [10], the collision cross sections can be controlled by manipulating the character of the initial coherent superposition states in which the molecules are prepared.

In this paper we examine the coherent control of identical particle scattering in detail, with para-H₂ + para-H₂ as an example. In doing so we approach this issue from a different perspective from that in our earlier work [10], demonstrating deep connections to the construction and use of *entangled states*, a topic of great recent interest in quantum information science [11]. That is, we show that the scattering amplitudes, and the resultant differential and total collision cross sections, depend strongly on quantum entanglement embedded in the initial rovibrational state. In essence, entanglement-induced quantum effects are shown to occur without the explicit preparation of entangled states. This provides a novel means of controlling both the the differential and total collision cross sections in identical diatom-diatom scattering.

* Permanent address: Chemical Physics Department, The Weizmann Institute of Science, Rehovot, Israel 76100

This paper is organized as follows. In Sec. II, we introduce some concepts related to quantum entanglement between identical particles and then address the theory of identical diatom-diatom scattering with particular reference to entangled molecular rovibrational states as the incoming asymptotic states. The theoretical formalism is presented in Sec. III for para-H₂ + para-H₂ system, without loss of much generality. Results for the scattering of this system are shown in Sec. IV where detailed computational results on the role of entangled rovibrational states in both elastic and inelastic scattering, with the collision energy ranging from 400 cm⁻¹ to the ultracold regime, are explored. A discussion is provided in Sec. V.

II. AB + AB SCATTERING

A. Identical Particle Entanglement

Quantum entanglement is a striking feature of quantum physics. Qualitatively, two particles are said to be quantum entangled if their total wavefunction is inseparable. In particular, if two particles are entangled then neither of them possesses a complete set of properties, since measuring one of them would collapse the total wavefunction and thus affect the properties of the other. Quantum entanglement is a fundamental issue of considerable theoretical interest, and plays a key role in various modern areas such as quantum teleportation [12, 13], quantum cryptography, and quantum computing [11].

In the case of identical particles the total wavefunction, including all degrees of freedom, is always symmetrized or anti-symmetrized with respect to particle exchange. Hence, even if the total wavefunction of two identical particles is simply obtained by symmetrizing (or anti-symmetrizing) a separable state, it appears to be unfactorizable, and hence apparently entangled. This is, in fact, misleading and hints that quantum entanglement between identical particles is somewhat more subtle than quantum entanglement between non-identical particles. In a recent discussion, Ghirardi et al [14] have given clear definitions of quantum entanglement between two identical particles: (i) two identical fermions are entangled if the total wavefunction cannot be obtained by anti-symmetrizing a factorized state, and (ii) two identical bosons are entangled if the total wavefunction cannot be obtained by symmetrizing a factorized product of two orthogonal states and if the total wavefunction is not a product of the same state for the two particles. Under these circumstances, the state is entangled and each of the particle pairs does not possess a full set of properties.

One intriguing aspect of quantum entanglement between identical particles, relevant to the discussion below, is that it can force different permutation symmetries on some degrees of freedom. For example, consider a system of two freely moving identical spin 1/2 particles, whose spin up and spin down states are represented by $|\uparrow_1\rangle$, $|\downarrow_1\rangle$, $|\uparrow_2\rangle$, $|\downarrow_2\rangle$. If the total spin is zero, then the two spins are entangled and the resulting (“EPR state”) $|\psi\rangle$ is given by

$$|\psi\rangle = \frac{1}{\sqrt{2}}(|\uparrow_1\rangle \otimes |\downarrow_2\rangle - |\downarrow_1\rangle \otimes |\uparrow_2\rangle). \quad (1)$$

Note that $|\psi\rangle$ in Eq. (1) cannot be obtained by anti-symmetrizing a factorizable *total* wavefunction (since such an anti-symmetrized state should also describe the translational motion) of two spin 1/2 particles. Clearly, $|\psi\rangle$ in Eq. (1) acquires a factor of -1 upon permutation. Since the permutation symmetry for the total wavefunction including all degrees of freedom is -1 for identical fermions, the permutation symmetry of the spatial degrees of freedom must be $+1$. Thus, in a simple bound system such as para-H₂, the rotational quantum number has to be even. Likewise, in unbound cases such as electron-electron or proton-proton scattering, the differential cross sections do depend strongly on how the two spins are entangled, even if the scattering potential is spin independent, e.g., a pure Coulomb potential [15]. This selection of specific permutation symmetry combinations due to entanglement of a subset of the system degrees of freedom is central to the results below.

B. The Role of Entangled Rovibrational States in Identical Particle Scattering

Consider identical particle scattering. We focus on the diatom-diatom case AB + AB, but the considerations are general. If $|j, m, v\rangle$ denotes an eigenstate of the AB diatom with angular momentum quantum number j , angular momentum projection quantum number m and vibrational quantum number v , then a typical entangled ro-vibrational state of AB + AB is of the form

$$\begin{aligned} \langle \mathbf{r}_1, \mathbf{r}_2 | \psi(j_1 m_1 v_1 j_2 m_2 v_2) \rangle_{\alpha, \beta} &\equiv \cos(\alpha) \langle \mathbf{r}_1 | j_1, m_1, v_1 \rangle \langle \mathbf{r}_2 | j_2, m_2, v_2 \rangle \\ &+ \sin(\alpha) \exp(i\beta) \langle \mathbf{r}_1 | j_2, m_2, v_2 \rangle \langle \mathbf{r}_2 | j_1, m_1, v_1 \rangle. \end{aligned} \quad (2)$$

Of specific interest later below are the entangled states

$$|\psi(j_1 m_1 v_1 j_2 m_2 v_2)\rangle_{\pm} \equiv \frac{1}{\sqrt{2}}(\langle \mathbf{r}_1 | j_1, m_1, v_1 \rangle \langle \mathbf{r}_2 | j_2, m_2, v_2 \rangle \pm \langle \mathbf{r}_1 | j_2, m_2, v_2 \rangle \langle \mathbf{r}_2 | j_1, m_1, v_1 \rangle), \quad (3)$$

where the only distinction between the two states $|\psi(j_1 m_1 v_1 j_2 m_2 v_2)\rangle_{\pm}$ is the relative phase β (0 or π) between the two participating states $\langle \mathbf{r}_1 | j_1 m_1 v_1 \rangle \langle \mathbf{r}_2 | j_2 m_2 v_2 \rangle$ and $\langle \mathbf{r}_1 | j_2 m_2 v_2 \rangle \langle \mathbf{r}_2 | j_1 m_1 v_1 \rangle$. This difference is significant insofar as $|\psi(j_1 m_1 v_1 j_2 m_2 v_2)\rangle_+$ is invariant upon permutation of \mathbf{r}_1 and \mathbf{r}_2 , whereas $|\psi(j_1 m_1 v_1 j_2 m_2 v_2)\rangle_-$ acquires a factor of -1 upon permutation of \mathbf{r}_1 and \mathbf{r}_2 . It should be stressed that the permutation symmetry associated with $|\psi(j_1 m_1 v_1 j_2 m_2 v_2)\rangle_{\pm}$ has nothing to do with the permutation symmetry of the total wavefunction of identical particles, since the states $|\psi(j_1 m_1 v_1 j_2 m_2 v_2)\rangle_{\pm}$ describe only rotational and vibrational motion. Note also, for use later below, that entangled states $|\psi(j_1 m_1 v_1 j_2 m_2 v_2)\rangle_{\pm}$ also form a new set of basis states to describe a general entangled state, i.e.,

$$|\psi(j_1 m_1 v_1 j_2 m_2 v_2)\rangle_{\alpha, \beta} = \frac{\cos(\alpha) + \sin(\alpha) \exp(i\beta)}{\sqrt{2}} |\psi(j_1 m_1 v_1 j_2 m_2 v_2)\rangle_+ + \frac{\cos(\alpha) - \sin(\alpha) \exp(i\beta)}{\sqrt{2}} |\psi(j_1 m_1 v_1 j_2 m_2 v_2)\rangle_-. \quad (4)$$

Suppose that prior to the AB + AB collision the AB molecules (here labeled AB and AB' for convenience) are prepared, in accord with Ref. [10], in the superposition states:

$$\begin{aligned} |\psi_{AB}\rangle &= \cos(\alpha_1) |j_1 m_1 v_1\rangle + \sin(\alpha_1) \exp(i\beta_1) |j_2 m_2 v_2\rangle \\ |\psi_{AB'}\rangle &= \cos(\alpha_2) |j_1 m_1 v_1\rangle + \sin(\alpha_2) \exp(i\beta_2) |j_2 m_2 v_2\rangle \end{aligned} \quad (5)$$

Then the total internal wavefunction (before symmetrization) is a direct product $|\psi_{dp}\rangle$ of these two superposition states, rather than an entangled molecular state. Nevertheless, $|\psi_{dp}\rangle$ can be expressed in terms of an entangled state plus two additional components, i.e.,

$$\begin{aligned} |\psi_{dp}\rangle &= y \exp(i\beta_2) |\psi(j_1 m_1 v_1 j_2 m_2 v_2)\rangle_{\alpha\beta} + \cos(\alpha_1) \cos(\alpha_2) |j_1 m_1 v_1\rangle \otimes |j_1 m_1 v_1\rangle \\ &\quad + \sin(\alpha_1) \sin(\alpha_2) \exp[i(\beta_1 + \beta_2)] |j_2 m_2 v_2\rangle \otimes |j_2 m_2 v_2\rangle, \end{aligned} \quad (6)$$

where the entangled state component $|\psi(j_1 m_1 v_1 j_2 m_2 v_2)\rangle_{\alpha\beta}$ is given by Eq. (4), with

$$\begin{aligned} y &= \sqrt{\cos^2(\alpha_1) \sin^2(\alpha_2) + \sin^2(\alpha_1) \cos^2(\alpha_2)}, \\ \alpha &= \cos^{-1}[\cos(\alpha_1) \sin(\alpha_2)/y], \\ \beta &= \beta_1 - \beta_2, \end{aligned} \quad (7)$$

and the two additional components $|j_1 m_1 v_1\rangle \otimes |j_1 m_1 v_1\rangle$ and $|j_2 m_2 v_2\rangle \otimes |j_2 m_2 v_2\rangle$ are called, in the spirit of previous coherent control work, ‘‘satellite’’ states [10]. From this viewpoint, the contribution from the entangled state component is the control term.

If our interest is in coherent control of AB + AB scattering, then this provides an obvious route to control. That is, by altering the α_i and β_i in the prepared diatomic state, one can alter the initial state. This introduces controllable quantum interferences, as previously discussed [10], hence altering product cross sections.

Alternatively, if our interest is in the dynamics of entangled states then collisions of AB + AB in the prescribed initial states may well provide a route to directly observing entanglement-induced quantum effects. Specifically, there clearly are cases, some cited in computations below, where contributions from the entangled molecular state dominate over that of the satellite states. That is, for some channels characterized by j'_1, v'_1, j'_2, v'_2 , the scattering amplitude for the initial direct product state $|\psi_{dp}\rangle$ is entirely due to the $y \exp(i\beta_2) |\psi(j_1 m_1 v_1 j_2 m_2 v_2)\rangle_{\alpha\beta}$ component. For these cases, we have

$$\sigma(\theta, |\psi_{dp}\rangle) \approx y^2 \sigma(\theta, |\psi(j_1 m_1 v_1 j_2 m_2 v_2)\rangle_{\alpha\beta}), \quad (8)$$

where $\sigma(\theta, |\psi\rangle)$ represents the differential cross section summed over m'_1 and m'_2 and integrated over the azimuthal angle ϕ for the initial state $|\psi\rangle$. Alternatively, and more difficult to implement, if we restrict the measurement to a particular total energy of the product, contributions of the satellite states can be zero due to the energy restriction and the scattering becomes essentially that due to an initially entangled molecular state $|\psi(j_1 m_1 v_1 j_2 m_2 v_2)\rangle_{\alpha\beta}$. Thus,

significantly, in either case one can experimentally observe and utilize entanglement-assisted coherent control effects in diatom-diatom scattering without the difficult task of preparing entangled molecular states.

Below we develop a general description of the quantum effects associated with entanglement of molecular rovibrational motion in bimolecular scattering. We focus on the contribution from the entangled state since the remainder (i.e., the satellite terms) is ordinary scattering. In doing so we specifically study the scattering system para-H₂ + para-H₂, the simplest case of diatom-diatom scattering. Although many of the following arguments apply to both reactive and nonreactive scattering, we confine attention to elastic and inelastic scattering only.

III. SCATTERING FROM ENTANGLED ROVIBRATIONAL STATES: FORMALISM

Consider AB + AB scattering. We represent the vector pointing from the center of mass of the projectile to that of the target by \mathbf{R} , and the relative inter-atomic distance vectors of the two para-H₂ molecules by \mathbf{r}_1 and \mathbf{r}_2 , respectively. We use j_i, m_i, v_i ($i = 1, 2$) to denote the quantum numbers of angular momentum, the projection of angular momentum onto a space-fixed z axis, and vibrational motion, respectively, for each para-H₂ molecule. The fact that both the nuclear spin and the electronic spin of para-H₂ molecules are zero greatly simplifies the problem, while retaining the essence of physics. Note that each para-H₂ molecule (with electronic ground state) is a boson, so that the permutation symmetry of the total wavefunction $|\Psi(\mathbf{r}_1, \mathbf{r}_2, \mathbf{R})\rangle$ in the scattering problem is +1. That is,

$$|\Psi(\mathbf{r}_1, \mathbf{r}_2, \mathbf{R})\rangle = |\Psi(\mathbf{r}_2, \mathbf{r}_1, -\mathbf{R})\rangle. \quad (9)$$

As we shall see more clearly below, this implies that the parity of $|\Psi(\mathbf{r}_1, \mathbf{r}_2, \mathbf{R})\rangle$ with regard to \mathbf{R} depends on the permutation symmetry of the internal degrees of freedom \mathbf{r}_1 and \mathbf{r}_2 .

In traditional scattering, the initial state is characterized by $k, \hat{\mathbf{z}}, j_1, m_1, v_1, j_2, m_2, v_2$, and the final state characterized by $k', \hat{\mathbf{R}}, j'_1, m'_1, v'_1, j'_2, m'_2, v'_2$, where $\hbar k$ and $\hbar k'$ are the translational momenta for the initial and final states, with $k = k'$ ($k \neq k'$) in the case of elastic (inelastic) scattering. Below we exclude the case of $(j_1, m_1, v_1) = (j_2, m_2, v_2)$ as it does not allow for entanglement in rovibrational states. Since the colliding molecules are identical, both the incoming and the outgoing asymptotic states have to be appropriately symmetrized. However, to obtain the scattering amplitude it suffices to symmetrize either the incoming or outgoing state only [15]. If we choose to symmetrize the incoming state then the scattering amplitude is given by

$$\begin{aligned} & f(k' \hat{\mathbf{R}} j'_1 m'_1 v'_1 j'_2 m'_2 v'_2 \leftarrow k \hat{\mathbf{z}} j_1 m_1 v_1 j_2 m_2 v_2) \\ &= \tilde{f}(k' \hat{\mathbf{R}} j'_1 m'_1 v'_1 j'_2 m'_2 v'_2 \leftarrow k \hat{\mathbf{z}} j_1 m_1 v_1 j_2 m_2 v_2) \\ &+ \tilde{f}(k' \hat{\mathbf{R}} j'_1 m'_1 v'_1 j'_2 m'_2 v'_2 \leftarrow k(-\hat{\mathbf{z}}) j_2 m_2 v_2 j_1 m_1 v_1), \end{aligned} \quad (10)$$

where \tilde{f} represents the unsymmetrized scattering amplitudes under the assumption that the two molecules are distinguishable. Specifically, in terms of the T -matrix elements, we have [16, 17]

$$\begin{aligned} & \tilde{f}(k' \hat{\mathbf{R}} j'_1 m'_1 v'_1 j'_2 m'_2 v'_2 \leftarrow k \hat{\mathbf{z}} j_1 m_1 v_1 j_2 m_2 v_2) \\ &= \frac{i\sqrt{\pi}}{\sqrt{kk'}} \sum_{JMm'} \sum_{l j_{12} m_{12}} \sum_{l' j'_{12} m'_{12}} \sqrt{2l+1} i^{l-l'} Y_l^{m'}(\hat{\mathbf{R}}) C_{l' m' j'_{12} m'_{12}}^{JM} C_{l 0 j_{12} m_{12}}^{JM} \\ & \times C_{j'_1 m'_1 j'_2 m'_2}^{j'_{12} m'_{12}} C_{j_1 m_1 j_2 m_2}^{j_{12} m_{12}} T^{JM}(j'_1 v'_1 j'_2 v'_2 j'_{12} l' | j_1 v_1 j_2 v_2 j_{12} l), \end{aligned} \quad (11)$$

and

$$\begin{aligned} & \tilde{f}(k' \hat{\mathbf{R}} j'_1 m'_1 v'_1 j'_2 m'_2 v'_2 \leftarrow k(-\hat{\mathbf{z}}) j_2 m_2 v_2 j_1 m_1 v_1) \\ &= \frac{i\sqrt{\pi}}{\sqrt{kk'}} \sum_{JMm'} \sum_{l j_{12} m_{12}} \sum_{l' j'_{12} m'_{12}} (-1)^l \sqrt{2l+1} i^{l-l'} Y_l^{m'}(\hat{\mathbf{R}}) C_{l' m' j'_{12} m'_{12}}^{JM} C_{l 0 j_{12} m_{12}}^{JM} \\ & \times C_{j'_1 m'_1 j'_2 m'_2}^{j'_{12} m'_{12}} C_{j_2 m_2 j_1 m_1}^{j_{12} m_{12}} T^{JM}(j'_1 v'_1 j'_2 v'_2 j'_{12} l' | j_2 v_2 j_1 v_1 j_{12} l), \end{aligned} \quad (12)$$

where Y_l^m is the spherical function and $C_{j_1 m_1 j_2 m_2}^{j_{12} m_{12}}$ are the Clebsch-Gordan coefficient.

Consider now the case where the molecules are initially prepared in an entangled state of molecular rovibrational states (as in the cross term in Eq. (6)): $\langle \mathbf{r}_1, \mathbf{r}_2 | \psi(j_1 m_1 v_1 j_2 m_2 v_2) \rangle_{\alpha, \beta}$. The two components of $|\psi(j_1 m_1 v_1 j_2 m_2 v_2) \rangle_{\alpha, \beta}$ shown in Eq. (2) are degenerate in energy. Hence they can interfere with each other, providing interference effects that allow for control.

To simplify matters we focus on the role of the entangled states $|\psi(j_1 m_1 v_1 j_2 m_2 v_2)\rangle_{\pm}$. Consideration of three special cases is in order:

(a) $j_1 = j_2, v_1 = v_2, m_1 \neq m_2$. Here

$$|\psi(j_1 m_1 v_1 j_2 m_2 v_2)\rangle_{\pm} = \frac{1}{\sqrt{2}}(|m_1\rangle|m_2\rangle \pm |m_2\rangle|m_1\rangle) \otimes |j_1, v_1\rangle \otimes |j_2, v_2\rangle. \quad (13)$$

In this case entanglement arises only through molecular rotation motion along a space fixed axis. Case (a) is therefore totally analogous to two entangled spins [see Eq. (1)]. Indeed, quantum effects arising from such entanglement can also be understood in terms of polarization phenomena, in accord with general polarization theory [18].

(b) $m_1 = m_2, j_1 = j_2, v_1 \neq v_2$. In this case we have

$$|\psi(j_1 m_1 v_1 j_2 m_2 v_2)\rangle_{\pm} = \frac{1}{\sqrt{2}}(|v_1\rangle|v_2\rangle \pm |v_2\rangle|v_1\rangle) \otimes |m_1, j_1\rangle \otimes |m_2, j_2\rangle. \quad (14)$$

Here only vibrational motion is entangled; rotational motion is completely separable. Further, unlike case (a), the resulting quantum entanglement is entirely due to internal excitation.

(c) $m_1 = m_2, v_1 = v_2, j_1 \neq j_2$. Thus,

$$|\psi(j_1 m_1 v_1 j_2 m_2 v_2)\rangle_{\pm} = \frac{1}{\sqrt{2}}(|j_1\rangle|j_2\rangle \pm |j_2\rangle|j_1\rangle) \otimes |m_1, v_1\rangle \otimes |m_2, v_2\rangle. \quad (15)$$

This case is somewhat complicated. Equation (15) implies that, while vibrational motion is not entangled, rotational degrees of freedom are partially entangled, insofar as the motion along a space fixed axis is still separable. Note that in this case quantum entanglement is also due to internal excitation, and that it is intrinsically different from case (a) and unrelated to any description based on polarization theory.

Using Eqs. (10) and (3), one obtains the following scattering amplitude $f_{\pm}(\hat{\mathbf{R}})$ from the initial entangled state $(k, \hat{\mathbf{z}}, |\psi(j_1 m_1 v_1 j_2 m_2 v_2)\rangle_{\pm})$ to the final state $k', \hat{\mathbf{R}}, j'_1, m'_1, v'_1, j'_2, m'_2, v'_2$:

$$\begin{aligned} f_{\pm}(\hat{\mathbf{R}}) &= \frac{1}{\sqrt{2}} \tilde{f}(k' \hat{\mathbf{R}} j'_1 m'_1 v'_1 j'_2 m'_2 v'_2 \leftarrow k \hat{\mathbf{z}} j_1 m_1 v_1 j_2 m_2 v_2) \\ &\quad + \frac{1}{\sqrt{2}} \tilde{f}(k' \hat{\mathbf{R}} j'_1 m'_1 v'_1 j'_2 m'_2 v'_2 \leftarrow k(-\hat{\mathbf{z}}) j_2 m_2 v_2 j_1 m_1 v_1) \\ &\quad \pm \frac{1}{\sqrt{2}} \tilde{f}(k' \hat{\mathbf{R}} j'_1 m'_1 v'_1 j'_2 m'_2 v'_2 \leftarrow k \hat{\mathbf{z}} j_2 m_2 v_2 j_1 m_1 v_1) \\ &\quad \pm \frac{1}{\sqrt{2}} \tilde{f}(k' \hat{\mathbf{R}} j'_1 m'_1 v'_1 j'_2 m'_2 v'_2 \leftarrow k(-\hat{\mathbf{z}}) j_1 m_1 v_1 j_2 m_2 v_2). \end{aligned} \quad (16)$$

Integrating $|f_{\pm}(\hat{\mathbf{R}})|^2$ over $\hat{\mathbf{R}}$ gives $|f_{\pm}|^2$, which is proportional to the cross section for the $j'_1 m'_1 v'_1 j'_2 m'_2 v'_2 \leftarrow j_1 m_1 v_1 j_2 m_2 v_2$ transition, with the initial state given by the plus or minus combination. The square of the amplitude for the same transition integrated over $\hat{\mathbf{R}}$, but from the collision where the initial state is $AB(j_1 m_1 v_1) + AB(j_2 m_2 v_2)$ [properly symmetrized] is given by $|f|^2$. Then, using Eqs. (10) and (16) we have that

$$|f|^2 = \frac{|f_+|^2 + |f_-|^2}{2}. \quad (17)$$

By comparing $|f_+|^2$, $|f_-|^2$ and $|f|^2$ we can ascertain the effect of entangling rovibrational states, and ascertain the degree of control.

Given Eqs. (11), (12) and (16), the $f_{\pm}(\hat{\mathbf{R}})$ can be written as:

$$\begin{aligned} f_{\pm}(\hat{\mathbf{R}}) &= \frac{1}{\sqrt{2}} \frac{i\sqrt{\pi}}{\sqrt{k k'}} \sum_{JMm'} \sum_{l j_1 m_1 m_2} \sum_{l' j'_1 m'_1 m'_2} \sqrt{2l+1} i^{l-l'} Y_{l'}^{m'}(\hat{\mathbf{R}}) C_{l' m' j'_1 m'_1 m'_2}^{JM} C_{l 0 j_1 m_1 m_2}^{JM} C_{j'_1 m'_1 j'_2 m'_2}^{j'_1 m'_1} \\ &\quad \times \{ [1 \pm (-1)^l] [C_{j_1 m_1 j_2 m_2}^{j_1 m_1} T^{JM}(j'_1 v'_1 j'_2 v'_2 j'_1 l' | j_1 v_1 j_2 v_2 j_1 l) \\ &\quad \pm C_{j_2 m_2 j_1 m_1}^{j_2 m_2} T^{JM}(j'_1 v'_1 j'_2 v'_2 j'_1 l' | j_2 v_2 j_1 v_1 j_1 l)] \}. \end{aligned} \quad (18)$$

Equation (18) suggests that there are two important quantum effects in $AB + AB$ scattering associated with using entangled molecular states as initial states: (1) Due to the factor $[1 \pm (-1)^l]$, the permutation symmetry induced by molecular entanglement imposes a parity restriction on the incoming partial waves. That

is, for the case of $|\psi(j_1 m_1 v_1 j_2 m_2 v_2)\rangle_+$ ($|\psi(j_1 m_1 v_1 j_2 m_2 v_2)\rangle_-$), contributions from odd (even) partial waves are completely suppressed, whereas contributions from even (odd) partial waves are enhanced. For example, for the case of $|\psi(j_1 m_1 v_1 j_2 m_2 v_2)\rangle_-$, although the two para- H_2 molecules are spinless bosons, they avoid the $l = 0$ state due to quantum entanglement of rovibrational motion. (2) As indicated by the factor $[C_{j_1 m_1 j_2 m_2}^{j_1' m_1' j_2' m_2'} T^{JM}(j_1' v_1' j_2' v_2' j_{12}' l' | j_1 v_1 j_2 v_2 j_{12} l) \pm C_{j_2 m_2 j_1 m_1}^{j_1' m_1' j_2' m_2'} T^{JM}(j_1' v_1' j_2' v_2' j_{12}' l' | j_2 v_2 j_1 v_1 j_{12} l)]$ in Eq. (18), there is quantum interference between transitions $(j_1 v_1 j_2 v_2 j_{12} l) \rightarrow (j_1' v_1' j_2' v_2' j_{12}' l')$ and $(j_2 v_2 j_1 v_1 j_{12} l) \rightarrow (j_1' v_1' j_2' v_2' j_{12}' l')$. Whether this interference is constructive or destructive depends on the form of the entangled rovibrational state. This effect is significant when the magnitude of $T^{JM}(j_1' v_1' j_2' v_2' j_{12}' l' | j_1 v_1 j_2 v_2 j_{12} l)$ is comparable to that of $T^{JM}(j_1' v_1' j_2' v_2' j_{12}' l' | j_2 v_2 j_1 v_1 j_{12} l)$. Further, based on Eq. (18), the scattering amplitude $f_{\alpha,\beta}(\hat{\mathbf{R}})$ for an arbitrary incoming entangled state $(k, \hat{\mathbf{z}}, |\psi(j_1 m_1 v_1 j_2 m_2 v_2)\rangle_{\alpha,\beta})$ can then be expressed as

$$f_{\alpha,\beta}(\hat{\mathbf{R}}) = \frac{\cos(\alpha) + \sin(\alpha) \exp(i\beta)}{\sqrt{2}} f_+(\hat{\mathbf{R}}) + \frac{\cos(\alpha) - \sin(\alpha) \exp(i\beta)}{\sqrt{2}} f_-(\hat{\mathbf{R}}). \quad (19)$$

As mentioned above, an alternative but equivalent way to symmetrize the scattering amplitude is to symmetrize the outgoing asymptotic state. That is,

$$\begin{aligned} & f(k' \hat{\mathbf{R}} j_1' m_1' v_1' j_2' m_2' v_2' \leftarrow k \hat{\mathbf{z}} j_1 m_1 v_1 j_2 m_2 v_2) \\ &= \tilde{f}(k' \hat{\mathbf{R}} j_1' m_1' v_1' j_2' m_2' v_2' \leftarrow k \hat{\mathbf{z}} j_1 m_1 v_1 j_2 m_2 v_2) \\ & \quad + \tilde{f}(k' (-\hat{\mathbf{R}}) j_2' m_2' v_2' j_1' m_1' v_1' \leftarrow k \hat{\mathbf{z}} j_1 m_1 v_1 j_2 m_2 v_2). \end{aligned} \quad (20)$$

Based on this procedure, we have

$$\begin{aligned} f_{\pm}(\hat{\mathbf{R}}) &= \frac{1}{\sqrt{2}} \tilde{f}(k' \hat{\mathbf{R}} j_1' m_1' v_1' j_2' m_2' v_2' \leftarrow k \hat{\mathbf{z}} j_1 m_1 v_1 j_2 m_2 v_2) \\ & \quad + \frac{1}{\sqrt{2}} \tilde{f}(k' (-\hat{\mathbf{R}}) j_2' m_2' v_2' j_1' m_1' v_1' \leftarrow k \hat{\mathbf{z}} j_1 m_1 v_1 j_2 m_2 v_2) \\ & \quad \pm \frac{1}{\sqrt{2}} \tilde{f}(k' \hat{\mathbf{R}} j_1' m_1' v_1' j_2' m_2' v_2' \leftarrow k \hat{\mathbf{z}} j_2 m_2 v_2 j_1 m_1 v_1) \\ & \quad \pm \frac{1}{\sqrt{2}} \tilde{f}(k' (-\hat{\mathbf{R}}) j_2' m_2' v_2' j_1' m_1' v_1' \leftarrow k \hat{\mathbf{z}} j_2 m_2 v_2 j_1 m_1 v_1). \end{aligned} \quad (21)$$

In terms of the partial wave expansion, the scattering amplitude $f_{\pm}(\hat{\mathbf{R}})$ in Eq. (21) can be further expressed as

$$\begin{aligned} f_{\pm}(\hat{\mathbf{R}}) &= \frac{1}{\sqrt{2}} \frac{i\sqrt{\pi}}{\sqrt{k k'}} \sum_{JMm'} \sum_{l j_{12} m_{12}} \sum_{l' j_{12}' m_{12}'} \sqrt{2l+1} i^{l-l'} C_{l' m' j_{12}' m_{12}'}^{JM} C_{l 0 j_{12} m_{12}}^{JM} \\ & \quad \times \{ C_{j_1 m_1 j_2 m_2}^{j_1' m_1' j_2' m_2'} [C_{j_1' m_1' j_2' m_2'}^{j_{12}' m_{12}'} Y_{l'}^{m'}(\hat{\mathbf{R}}) T^{JM}(j_1' v_1' j_2' v_2' j_{12}' l' | j_1 v_1 j_2 v_2 j_{12} l) \\ & \quad + C_{j_2' m_2' j_1' m_1'}^{j_{12}' m_{12}'} Y_{l'}^{m'}(-\hat{\mathbf{R}}) T^{JM}(j_2' v_2' j_1' v_1' j_{12}' l' | j_1 v_1 j_2 v_2 j_{12} l)] \\ & \quad \pm C_{j_2 m_2 j_1 m_1}^{j_{12} m_{12}} [C_{j_1' m_1' j_2' m_2'}^{j_{12}' m_{12}'} Y_{l'}^{m'}(\hat{\mathbf{R}}) T^{JM}(j_1' v_1' j_2' v_2' j_{12}' l' | j_2 v_2 j_1 v_1 j_{12} l) \\ & \quad \pm C_{j_2' m_2' j_1' m_1'}^{j_{12}' m_{12}'} Y_{l'}^{m'}(-\hat{\mathbf{R}}) T^{JM}(j_2' v_2' j_1' v_1' j_{12}' l' | j_2 v_2 j_1 v_1 j_{12} l)] \}. \end{aligned} \quad (22)$$

Interestingly, the equivalence of Eq. (22) with Eq. (18) is far from obvious [19]. As a result, we can no longer readily identify the parity restriction imposed on the incoming partial waves due to molecular entanglement. In this sense, in the theoretical considerations, we prefer Eq. (18) to Eq. (22). However, Eq. (22) is very useful in order to confirm the consistency of our results. For all computational examples presented below we have verified that Eqs. (18) and (22) give the same results.

IV. CALCULATIONS AND RESULTS

In this section we focus on computations for case (c) described above. Specifically, we consider rotational energy transfer in rotor-rotor scattering, a problem that has been the subject of considerable interest [16, 17]. We do not treat case (a) since it is an example of well-known polarization theory. Case (b), on the other hand, requires computations

beyond current capabilities. However, to provide some insight into this case we do present results for one case (b) *model*. That is, we treat a lower dimensional case of vibrational excitation with frozen rotational motion.

MOLSCAT [20] is a useful tool for this study. In particular, it provides both cross sections and S -matrix elements necessary for the study of phase control. MOLSCAT also introduces a control parameter to account for whether or not the scattering particles are identical. Thus, we can first assume that the two scattering molecules are distinguishable and compute all the matrix elements $T^{JM}(j'_1 v'_1 j'_2 v'_2 j'_1 l' | j_1 v_1 j_2 v_2 j_1 l)$ and $T^{JM}(j'_1 v'_1 j'_2 v'_2 j'_1 l' | j_2 v_2 j_1 v_1 j_1 l)$, and then use Eq. (18) to calculate the cross sections. The Zarur-Rabitz interaction potential [21] for para- $\text{H}_2 + \text{para-}\text{H}_2$ is used throughout; it certainly suffices for the demonstration of novel quantum effects in bimolecular scattering. However, newer global potentials are available for $\text{H}_2 + \text{H}_2$ scattering [22] that can be used for detailed comparisons with future experimental studies.

A. Scattering at $E_k = 400, 40, 4 \text{ cm}^{-1}$

To demonstrate the role of entanglement we consider scattering for different incoming entangled molecular states at collision energies $E_k = 400, 40,$ and 4 cm^{-1} . In particular, $E_k = 400 \text{ cm}^{-1}$ ($\approx 570^\circ \text{ K}$) is still below the vibration excitation threshold, and $E_k = 4 \text{ cm}^{-1}$ ($\approx 5.7^\circ \text{ K}$) is very close to the lowest collision temperature currently achievable in molecular crossed-beam experiments.

We consider the following entangled molecular states in our computations:

$$|\psi_{j_1 j_2}^\pm\rangle = \frac{1}{\sqrt{2}}(|j_1\rangle|j_2\rangle \pm |j_2\rangle|j_1\rangle) \otimes |m_1 = 0, v_1 = 0\rangle \otimes |m_2 = 0, v_2 = 0\rangle. \quad (23)$$

Subsequent computational investigation [23] of other α, β values in Eq. (4) confirmed that these two states give the control extremes.

Since we consider rotational excitation only, all vibrational quantum numbers are set to be zero, i.e., $v_1 = v_2 = v'_1 = v'_2 = 0$. In a typical experiment one might well prepare the AB diatomic superposition state by laser excitation of $|j_1, m_1, v_1\rangle$ to $|j_2, m_2, v_2\rangle$. Assuming linearly polarized light, selection rules ensure that $m_1 = m_2$. However, as long as $m_1 = m_2$ (so that we can not distinguish between the two scattering molecules by measuring the projection of their angular momentum), the results for all m are essentially the same. Hence, here we consider $m_1 = m_2 = 0$.

Figure 1 shows the θ dependence of the elastic differential cross section $\sigma_e(\theta)$ summed over the final-state quantum numbers m'_1 and m'_2 and integrated over the azimuthal angle ϕ ($\mathbf{R} \equiv (\theta, \phi)$), for the two incoming entangled states $|\psi_{j_1 j_2}^\pm\rangle$ with $j_1 = 2, j_2 = 0$. In particular, E_k equals 400 cm^{-1} in Fig. 1a, 40 cm^{-1} in Fig. 1b, and 4 cm^{-1} in Fig. 1c. For all three cases there is a clear difference in $\sigma_e(\theta)$ between the $|\psi_{j_1 j_2}^+\rangle$ and $|\psi_{j_1 j_2}^-\rangle$ cases. Indeed, for particular scattering angles, e.g., for θ close to $\pi/2$, molecular entanglement induces huge differences. Also evident is that the number of minima of $\sigma_e(\theta)$ is always even (odd) for $|\psi_{j_1 j_2}^+\rangle$ ($|\psi_{j_1 j_2}^-\rangle$), a manifestation of the parity restriction of the incoming partial waves resulting from the permutation symmetry of the entangled molecular states. Further, comparing Fig. 1c with Fig. 1a and Fig. 1b, it is clear that lower collision energy induces slower oscillations in $\sigma_e(\theta)$. This is expected due to the behavior of $Y_l^{m'}(\mathbf{R})$ in Eq. (18).

Consider then the total cross section σ_e for elastic scattering, denoted σ_e^\pm for the $|\psi_{j_1 j_2}^\pm\rangle$ cases. Integrating $\sigma_e(\theta)$ over θ for the lowest energy case (Fig. 1c) gives $\sigma_e^+ = 511 \text{ \AA}^2$ and $\sigma_e^- = 346 \text{ \AA}^2$. This is to be compared to the total elastic cross section for scattering of $\text{AB}(j = 0, m = 0) + \text{AB}(j = 2, m = 0)$, proportional to $|f|^2$ summed over m'_1 and m'_2 , denoted σ_e and equal to 428 \AA^2 . If we define the percentage of control in this case as $d_c = |100(\sigma_e^+ - \sigma_e^-)/\sigma_e|$ then $d_c = 39\%$. For the other two higher energy cases (see Fig. 1a and Fig. 1b) the cross sections are found to be less sensitive to the quantum entanglement in the incoming state, with $d_c = 5\%$ and 13% , respectively. Note also that the probability of the direct transition $j_1 = 2, j_2 = 0 \rightarrow j'_1 = 2, j'_2 = 0$ is much larger than that of the exchange transition $j_1 = 0, j_2 = 2 \rightarrow j'_1 = 2, j'_2 = 0$. Thus, the effect from the quantum interference between the scattering amplitudes $T^{JM}(20002l'|20002l)$ and $T^{JM}(20002l'|00202l)$ [see Eq. (18)] is negligible. As a result, quantum features observed in Fig. 1 are entirely due to the first quantum effect identified in the previous section, i.e., the partial-wave parity selection effect.

In Fig. 2, we show inelastic differential cross sections $\sigma_i(\theta)$ summed over m'_1 and m'_2 and integrated over the angle ϕ , for the incoming entangled states $|\psi_{j_1 j_2}^\pm\rangle$, with initial-state quantum numbers $j_1 = 4, j_2 = 0$, and final-state quantum numbers $j'_1 = j'_2 = 2$. The collision energy E_k equals 400 cm^{-1} in Fig. 2a, 40 cm^{-1} in Fig. 2b, and 4 cm^{-1} in Fig. 2c. For these initial-state and final-state channels, the T -matrix elements contributing to the cross sections are $T^{JM}(2020j'_{12}l'|40004l)$ and $T^{JM}(2020j'_{12}l'|00404l)$ [see Eq. (18)]. A careful examination of these T -matrix elements shows that

$$T^{JM}(2020j'_{12}l'|40004l) = (-1)^{j'_{12}} T^{JM}(2020j'_{12}l'|00404l). \quad (24)$$

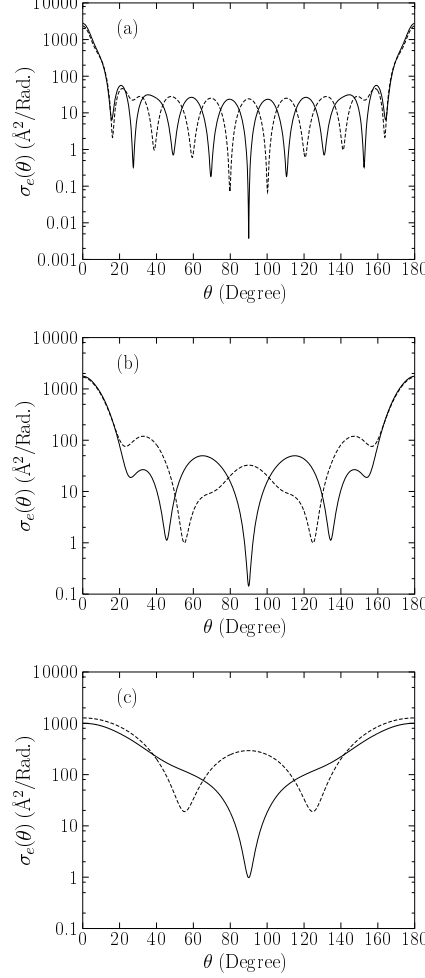


FIG. 1: The θ dependence of the elastic differential cross section summed over the final state quantum numbers m'_1 and m'_2 and integrated over ϕ . The scattering system is para- $\text{H}_2 + \text{para-}\text{H}_2$, and the collision energy is (a) 400 cm^{-1} ($\approx 570^\circ \text{ K}$), (b) 40 cm^{-1} ($\approx 57^\circ \text{ K}$), and (c) 4 cm^{-1} ($\approx 5.7^\circ \text{ K}$). Dashed and solid lines are for the incoming free entangled states $|\psi_{j_1 j_2}^+\rangle$ and $|\psi_{j_1 j_2}^-\rangle$ [see Eq. (23)], respectively. Here $j_1 = 2$, $j_2 = 0$.

Hence, the second quantum effect described by Eq. (18), i.e., quantum interference between $T^{JM}(2020j'_{12}l'|40004l)$ and $T^{JM}(2020j'_{12}l'|00404l)$, also becomes important. Indeed, our choice of the final-state channel as $j'_1 = j'_2$ is motivated by the fact that for $j'_1 \neq j'_2$, the second quantum effect is insignificant. As seen in Fig. 2, different incoming entangled states cause different oscillatory $\sigma_i(\theta)$ patterns, leading to large differences in $\sigma_i(\theta)$ for fixed scattering angle (e.g., for θ close to 0 or π in Fig. 2b and Fig. 2c, and for θ around $\pi/2$ in Fig. 2b). In comparing Figs. 2a, 2b and 2c, one sees that in the highest collision energy case, quantum effects are least significant. This trend is similar to the elastic scattering case, and can also be understood via Eq. (18). In particular, using Eq. (24) and the fact that the total parity is always conserved, Eq. (18) can be further reduced to

$$\begin{aligned}
 f_{\pm}(\hat{\mathbf{R}}) &= \frac{1}{\sqrt{2}} \frac{i\sqrt{\pi}}{\sqrt{k k'}} \sum_{Jn l' j'_{12} m'_{12}} \sqrt{2l+1} (-1)^n Y_{l+2n}^{-m'_{12}}(\hat{\mathbf{R}}) C_{(l+2n)(-m'_{12})j'_{12}m'_{12}}^{J0} C_{l040}^{J0} C_{2m'_{12}m'_{12}}^{j'_{12}m'_{12}} \\
 &\quad \times C_{4000}^{40} [1 \pm (-1)^l] T^{J0}(2020j'_{12}(l+2n)|40004l) [1 + (-1)^{l+j'_{12}}], \tag{25}
 \end{aligned}$$

where $2n = l' - l$. Equations (24) and (25) show that quantum interference between $T^{J0}(2020j'_{12}l'|40004l)$ and $T^{J0}(2020j'_{12}l'|00404l)$ can also be interpreted as a selection rule imposed on the quantum number j'_{12} : for the incoming entangled state $|\psi_{40}^+\rangle$ only even incoming partial waves contribute and j'_{12} is restricted to be even, whereas for the

incoming entangled state $|\psi_{40}^- \rangle$, only odd incoming partial waves contribute and j'_{12} is restricted to be odd. This is consistent with the fact that the outgoing state is composed of two indistinguishable molecules, with the same rotational quantum number ($j'_1 = j'_2 = 2$).

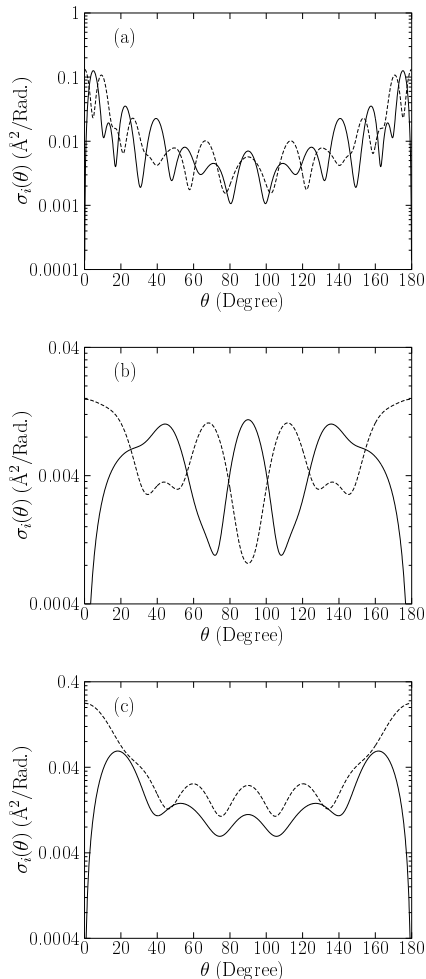


FIG. 2: The θ dependence of the inelastic differential cross section summed over the final state quantum numbers m'_1 and m'_2 and integrated over ϕ . The scattering system is para- $\text{H}_2 + \text{para-H}_2$, and the collision energy is (a) 400 cm^{-1} , (b) 40 cm^{-1} , and (c) 4 cm^{-1} . Dashed and solid lines are for the incoming free entangled states $|\psi_{j_1 j_2}^+ \rangle$ and $|\psi_{j_1 j_2}^- \rangle$ [see Eq. (23)], respectively. Here $j_1 = 4$, $j_2 = 0$, $j'_1 = j'_2 = 2$.

The case in Fig. 2c is worthy of further discussion. In this case one sees that $\sigma_i(\theta)$ for $|\psi_{j_1 j_2}^- \rangle$ (solid curve) is systematically smaller than that for $|\psi_{j_1 j_2}^+ \rangle$ (dashed curve), for almost the entire range of the scattering angle. This leads to a significant difference in the total inelastic cross section σ_i^\pm for the $|\psi_{j_1 j_2}^\pm \rangle$ cases: $\sigma_i^+ = 0.057 \text{ \AA}^2$ and $\sigma_i^- = 0.032 \text{ \AA}^2$, giving a control range of $d_c = |100(\sigma_i^+ - \sigma_i^-)/\sigma_i| = 57\%$, where σ_i is the total inelastic cross section for scattering from $\text{AB}(j = 4, m = 0) + \text{AB}(j = 0, m = 0)$ to the channel $j'_1 = j'_2 = 2$. However, d_c is less than 2% at the higher energies in Fig. 2. Thus, as in elastic scattering, total inelastic cross sections can also be sensitive to the quantum phase embedded in initial entangled molecular states at sufficiently low energies.

B. Ultracold Molecular Collisions: Extreme Quantum Effects

Given the results for $E_k > 5^\circ \text{ K}$, we consider ultracold collisions. This new area of focus, ultracold molecular scattering, has already displayed interesting quantum effects [24]. Further, understanding this area is also crucial in realizing molecular Bose-Einstein condensation [25, 26].

From the control point of view, the advantage of ultracold collisions is that scattering cross sections are often dominated by very few partial waves. This feature of ultracold collisions may well allow for new opportunities in manipulating molecular collisions [27]. For example, the fact that entangled incoming molecular states impose parity restrictions on the partial waves [see Eq. (18)] implies that quantum entanglement should be even more important at ultracold temperatures. Consider, for example, a zero collision energy limit case where only s-wave scattering ($l = 0$ partial wave) contributes to the cross sections [28]. In this case, if s-wave scattering is selected by molecular entanglement, the result would be enhanced nonzero cross sections. If s-wave scattering is forbidden due to molecular entanglement, then molecular scattering is completely suppressed. That is, in the elastic scattering case, all the scattering would be in the forward direction, and in the completely suppressed inelastic scattering case, there would be no inelastic scattering in any direction.

To confirm such theoretical considerations and to determine how cold the collisions need be in order to experimentally observe such extreme quantum effects, we extend our calculations to the ultracold regime, with E_k ranging from 0.4 cm^{-1} to 0.0004 cm^{-1} . These computations are generally easier than at higher energies because the maximum total angular momentum contributing to cross sections is very small [29].

Figure 3 shows $\sigma_e(\theta)$ for two energies [0.4 cm^{-1} and 0.04 cm^{-1}], with the incoming asymptotic states given by $|\psi_{j_1 j_2}^\pm\rangle$ ($j_1 = 2, j_2 = 0$). In both cases $\sigma_e(\theta)$ for $|\psi_{j_1 j_2}^+\rangle$ (dashed line) is fairly uniform suggesting that s-wave dominates the elastic scattering. Thus, preventing s-wave scattering via entanglement is expected to cause a dramatic decrease in the cross section. Indeed, in Fig. 3b, one sees that elastic scattering is almost totally suppressed for the $|\psi_{j_1 j_2}^-\rangle$ case. Integrating $\sigma_e(\theta)$ over θ gives $\sigma_e^+ = 724 \text{ \AA}^2$ and $\sigma_e^- = 285 \text{ \AA}^2$ with $d_c = 87\%$ for the case shown in Fig. 3a, and $\sigma_e^+ = 1014 \text{ \AA}^2$ and $\sigma_e^- = 11 \text{ \AA}^2$ with $d_c = 195\%$ for the case shown in Fig. 3b.

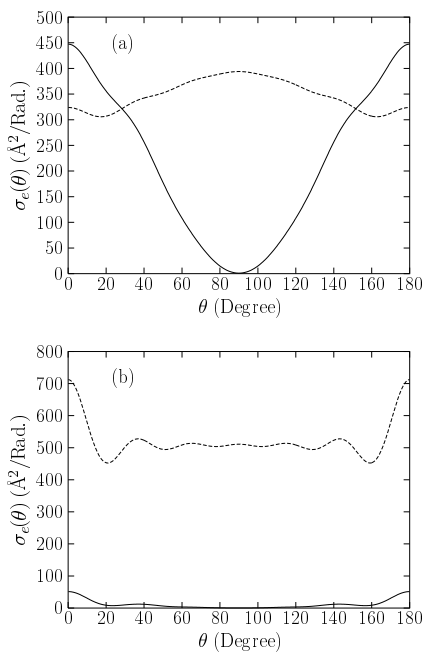


FIG. 3: As in Fig. 1 except that elastic collision is ultracold. The collision energy is (a) 0.4 cm^{-1} , and (b) 0.04 cm^{-1} .

Figure 4 shows sample results for ultracold inelastic scattering. As in Fig. 2, $|\psi_{j_1 j_2}^\pm\rangle$ ($j_1 = 4, j_2 = 0$) is chosen as the incoming asymptotic state and we examine transitions to $j_1' = 2, j_2' = 2$ with collision energies of 0.04 cm^{-1} and 0.0004 cm^{-1} . The differences in $\sigma_i(\theta)$ between $|\psi_{j_1 j_2}^+\rangle$ and $|\psi_{j_1 j_2}^-\rangle$ in Fig. 4a is somewhat similar to that in Fig. 2c, where the collision energy is 100 times larger, with a corresponding d_c of 22%. Hence, control is significant, but the system is insufficiently cold to show *extreme* quantum effects. By contrast, Fig. 4b shows results for the lowest E_k of 0.0004 cm^{-1} . Clearly, in this case, inelastic scattering for $|\psi_{j_1 j_2}^-\rangle$ is almost completely suppressed, whereas inelastic scattering for $|\psi_{j_1 j_2}^+\rangle$ remains significant. The integrated cross sections give $\sigma_i^+ = 1.63 \text{ \AA}^2$ and $\sigma_i^- = 0.02 \text{ \AA}^2$, with a $d_c = 194\%$.

Thus, we have demonstrated that quantum entanglement in the incoming asymptotic state can dramatically alter ultracold collision cross sections. These effects will also appear in the scattering of the superposition states in Eq.

(5). That is, Eq. (8) is well obeyed in all of the cases shown in Figs. 1 to 4. For example, in the elastic scattering case ($j_1 = 2, j_2 = 0, v_1 = v_2 = 0, m_1 = m_2 = 0, v'_1 = v'_2 = 0, j'_1 = 2, j'_2 = 0$) the scattering amplitude for the $j_1 = 2, j_2 = 2 \rightarrow j'_1 = 2, j'_2 = 0$ transition due to the first satellite state is orders of magnitude smaller than that for the $j_1 = 2, j_2 = 0 \rightarrow j'_1 = 2, j'_2 = 0$ transition associated with the entangled state term at the E_k considered. The probability of the transition $j_1 = 0, j_2 = 0 \rightarrow j'_1 = 2, j'_2 = 0$ due to the second satellite state is also negligible (indeed, it is exactly zero for $E_k < 364.8 \text{ cm}^{-1}$). Similarly, for the inelastic scattering case ($j_1 = 4, j_2 = 0, v_1 = v_2 = 0, m_1 = m_2 = 0, v'_1 = v'_2 = 0, j'_1 = 2, j'_2 = 2$), the scattering amplitude due to the first satellite, the de-excitation $j_1 = 4, j_2 = 4 \rightarrow j'_1 = 2, j'_2 = 2$, is negligible due to the large rotational energy mismatch between the initial and final channels. In addition, the second satellite state does not contribute to the product channel ($j'_1 = 2, j'_2 = 2$) for $E_k < 729.6 \text{ cm}^{-1}$.

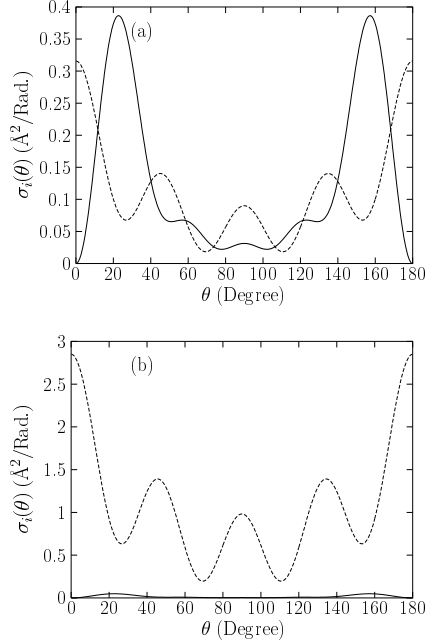


FIG. 4: As in Fig. 2 except that inelastic collision is ultracold. The collision energy is (a) 0.04 cm^{-1} , and (b) 0.0004 cm^{-1} .

Thus, for example if, in Eq. (8), $\alpha_1 = \alpha_2 = \pi/4$, then Eq. (8) reduces to

$$\begin{aligned} \sigma(\theta, |\psi_{dp}\rangle) &\approx \frac{1}{2} \sigma(\theta, |\psi_{j_1 j_2}^+\rangle), \quad \beta = 2n\pi; \\ \sigma(\theta, |\psi_{dp}\rangle) &\approx \frac{1}{2} \sigma(\theta, |\psi_{j_1 j_2}^-\rangle), \quad \beta = (2n + 1)\pi. \end{aligned} \quad (26)$$

In this case the role of β as a control parameter, evident in Eq. (26) as a method for switching between the plus and minus states, is worthy of note. For example, the elastic scattering results in Fig. 3b show that by varying β one can enhance, or almost completely suppress, the yield of the ($j'_1 = 2, j'_2 = 0$) channel in directions other than that of the incident momentum. Likewise, the inelastic scattering results in Fig. 4b suggest that by manipulating β we can enhance or almost shut off the ($j'_1 = 2, j'_2 = 2$) channel.

C. Vibrational Relaxation

The above discussion provides results on rotational energy transfer. The formalism, however, applies equally well to other types of scattering. Unfortunately, the current state-of-the-computational-art prevents a full quantum calculation on reactive scattering, or even on diatom-diatom rovibrational energy transfer. That is, the exact numerical treatment of $AB + AB$ in three dimensions is still not feasible and approximations such as the sudden approximation [30] may not be appropriate for low energy collisions of the type that we are examining since it assumes that molecular

rotation is slow compared with that of vibration and translation. Further, although a semiclassical treatment of rovibrational energy transfer is available [31] it ignores the role of the quantum effects in the translational motion. Nonetheless, we wish to gain some insight into phase control of vibrational relaxation. For this reason we present results on a simplified model of diatom-diatom scattering where the rotational motion is frozen. Specifically, we adopt a three-degree-of-freedom model that assumes that both the projectile and target molecules point at a fixed direction during the entire scattering process. The scattering problem is then computationally solved by wavepacket propagation. To do so we employ a time-dependent approach with real L^2 eigenfunctions with damping [32, 33].

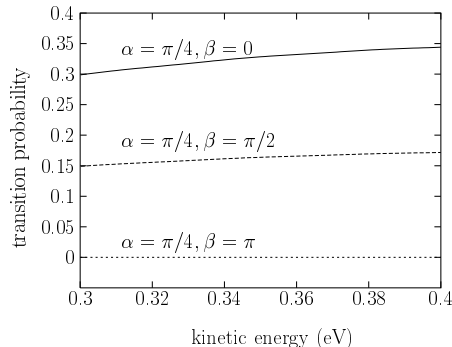


FIG. 5: The inelastic transition probability of the channel ($v'_1 = 1, v'_2 = 1$) versus the collision energy in the para- $\text{H}_2 + \text{para-}\text{H}_2$ scattering, for three incoming entangled vibrational states described by Eq. (27). $\alpha = \pi/4$, $\beta = 0$ (top curve), $\pi/2$ (middle curve) and π (bottom curve). The internuclear axis of each para- H_2 molecule is assumed to be parallel to the incident velocity during the scattering process.

Figure 5 displays the transition probability to the product ($v'_1 = 1, v'_2 = 1$) channel for three initial entangled vibrational states characterized by

$$\psi_{v_1 v_2}^{(\alpha, \beta)} = \cos(\alpha)|v_1 = 0\rangle \otimes |v_2 = 2\rangle + \exp(i\beta) \sin(\alpha)|v_1 = 2\rangle \otimes |v_2 = 0\rangle \quad (27)$$

with $\alpha = \pi/4$, $\beta = 0, \pi/2$, and π , respectively. As seen in Fig. 5, the quantum phase β embedded in the initial entangled vibrational states strongly affects vibration-vibration relaxation, with the cross section changing considerably as a function of the initial entangled state.

V. DISCUSSION AND SUMMARY

The results on para- $\text{H}_2 + \text{para-}\text{H}_2$ scattering make clear that entanglement can play a significant role in the control of nonreactive collisional processes. To investigate this phenomenon experimentally one could attempt to prepare the entangled molecular state directly. However, although quantum entanglement of atomic systems has been experimentally realized [34, 35], preparing entangled molecular states would require a considerable extension of technology. By contrast, contributions from entangled states appear naturally in the collision of AB + AB systems where the initial states are prepared as superpositions of the form given in Eq. (5). Preparing these states would entail excitation of the $|j_1, m_1, v_1\rangle$ to produce the superposition with $|j_2, m_2, v_2\rangle$. If the transition is dipole allowed then direct excitation of the lower state is possible. Alternatively, stimulated Raman adiabatic passage (STIRAP) [36] or the tripod-STIRAP scheme [37] may provide a useful choice for preparing the superposition states for both the projectile and the target molecules. In the latter approach an additional laser couples the intermediate level (through which the initial and final state are radiatively connected via the pump and Stokes-laser) with another unpopulated state. Depending on the time overlap of the additional laser with that of the pump and Stokes-laser, any coherent superposition state of the initial and final state can be created. Thus, by introducing different coherence characteristics from laser fields into the scattering system, we can control β and thus select the form of the entangled state component $|\psi_{dp}\rangle$ in Eq. (6), giving rise to phase control over differential and total cross sections.

Our studies have been restricted to nonreactive scattering of AB + AB, with particular numerical application to para- $\text{H}_2 + \text{para-}\text{H}_2$. As such, it remains to discuss the potential for applications to inelastic scattering of other systems and to comment on control of reactive scattering of identical particles.

General inelastic AB + AB scattering: Extensions to other inelastic scattering cases fall into two categories. The first are systems which, like para- $\text{H}_2 + \text{para-}\text{H}_2$, have zero total nuclear spin, zero total electronic orbital angular momentum, and zero total electronic spin. The theory of these cases is described above and is directly applicable

to inelastic scattering of other zero spin cases such as $CO + CO$, a system whose vibrational energy transfer is of interest in laser physics. However, the choice of zero spin merely simplifies theoretical considerations and it is not essential to control.

The second category, molecules with nonzero nuclear spin or electronic spin, does require an extension of the theory provided above. For such molecules, one of the two quantum effects due to entangled molecular states, i.e., the parity selection of the incoming partial waves, may be substantially reduced when the nuclear or electronic spin is unpolarized. To see this note that the spin degree of freedom can introduce additional permutation symmetries into the system. Thus, entangled rovibrational states like $|\psi(j_1 v_1 m_1 j_2 m_2 v_2)\rangle_{\pm}$ do not necessarily select the partial waves. For instance, for two unpolarized identical molecules with total integer nuclear spin I_N , the permutation symmetry of all other degrees of freedom is $+1$ with the probability $(I_N + 1)/(2I_N + 1)$ and -1 with the probability $(I_N)/(2I_N + 1)$ [17]. When I_N is large, two permutation symmetries of all other degrees of freedom are equally allowed. As a result, the permutation symmetry induced by entanglement of molecular rovibrational motion will have a negligible effect on the differential or total cross sections. However, as suggested in Ref. [10], one quantum effect still survives, i.e., quantum interference between the transition amplitudes $T^{JM}(j'_1 v'_1 j'_2 v'_2 j'_{12} l' | j_1 v_1 j_2 v_2 j_{12} l)$ and $T^{JM}(j'_1 v'_1 j'_2 v'_2 j'_{12} l' | j_2 v_2 j_1 v_1 j_{12} l)$. Establishing the magnitude of this effect alone will require further study.

Finally, note that there are considerable differences between the inelastic scattering case studied here and the case of reactive $AB + AB$ scattering (to form $A_2B + B$ or $A_2 + B_2$), the subject of future research. A full treatment of reactive scattering, which does require considerable extensions of current computational technique, is under consideration.

In summary, we have examined the nature of the interference, and hence control, in nonreactive $AB + AB$ scattering when the initial states are in a quantum superposition state. In doing so we have exposed the relationship of the interference term to entangled molecular rovibrational states as the incoming asymptotic state. Intriguing quantum effects resulting from quantum entanglement are revealed, and are shown to provide a novel means of controlling both nonreactive differential and total cross sections in identical diatom-diatom scattering.

Acknowledgments: The authors thank Dr. S. Skokov and Prof. J. Bowman for providing their scattering code (used for the vibrational relaxation case) employing the time-dependent approach with real L^2 eigenfunctions with damping. This work was supported by the U.S. Office of Naval Research and the Natural Sciences and Engineering Research Council of Canada.

-
- [1] M. Shapiro and P. Brumer, *Adv. Atom. Mol. and Opt. Phys.* **42**, 287 (2000); M. Shapiro and P. Brumer, *Principles of the Quantum Control of Molecular Processes* (John Wiley, New York, in press).
- [2] S.A. Rice and M. Zhao, *Optical Control of Molecular Dynamics* (John Wiley, New York, 2000).
- [3] H. Rabitz, R. de Vivie-Riedle, M. Motzkus, and K. Kompa, *Science* **288**, 824 (2000).
- [4] V. Sanchez-Villicana., S.D. Gensemer, K.Y.N. Tan, A. Kumarakrishnan, T.P. Dinneen, W. Suptitz, and P.L. Gould, *Phys. Rev. Lett.* **74**, 4619 (1995).
- [5] P.O. Fedichev, Yu. Kagan, G.V. Shlyapnikov, and J.T.M. Walraven, *Phys. Rev. Lett.* **77**, 2913 (1996).
- [6] M. Marinescu and L. You, *Phys. Rev. Lett.* **81**, 4596 (1998).
- [7] M. Shapiro and P. Brumer, *Phys. Rev. Lett.* **77**, 2574 (1996).
- [8] M. Shapiro and Y. Zeiri, *J. Chem. Phys.* **85**, 6449 (1986); T. Seideman and M. Shapiro, *J. Chem. Phys.*, **94**, 7910 (1991); A. Vardi and M. Shapiro, *Comm. At. Mol. Phys.* **2**, D233 (2001).
- [9] A. Abrashkevich, M. Shapiro, and P. Brumer, *Phys. Rev. Lett.* **81**, 3789 (1998); Erratum: *Phys. Rev. Lett.* **82**, 3002 (1999); *Faraday Discuss.* **113**, 291 (1999); E. Frishman, M. Shapiro, and P. Brumer, *J. Phys. Chem. A* **103**, 10333 (1999); A. Abrashkevich, M. Shapiro, and P. Brumer, *Chem. Phys.* **267**, 81 (2001).
- [10] P. Brumer, K. Bergmann, and M. Shapiro, *J. Chem. Phys.* **113**, 2053 (2000).
- [11] M.A. Nielsen and I.L. Chuang, *Quantum Computation and Quantum Information* (Cambridge University Press, Cambridge, 2000).
- [12] C.H. Bennett, G. Basare, C. Crépeau, R. Jozsa, A. Peres, and W.K. Wootters, *Phys. Rev. Lett.* **70**, 1895 (1993).
- [13] For a recent teleportation scenario based on entanglement in molecular dissociation and collisions, see T. Opatrny and G. Kurizki, *Phys. Rev. Lett.* **86**, 3180 (2000).
- [14] G. Ghirardi, L. Marinatto, and T. Weber, *J. Stat. Phys.* **108**, 49 (2002).
- [15] J.R. Taylor, *Scattering Theory* (Wiley, New York, 1972).
- [16] S. Green, *J. Chem. Phys.* **62**, 2271 (1975).
- [17] T.G. Heil, S. Green, and D.J. Kouri, *J. Chem. Phys.* **68**, 2562 (1978).
- [18] B.A. Robson, *The Theory of Polarization Phenomena* (Clarendon Press, Oxford, 1974).
- [19] To prove the equivalence between Eq. (22) and Eq. (18), one needs to use the fact that due to parity conservation, the T -matrix elements $T^{JM}(j'_1 v'_1 j'_2 v'_2 j'_{12} l' | j_1 v_1 j_2 v_2 j_{12} l)$ are nonzero only if $(-1)^{j_1+j_2+l} = (-1)^{j'_1+j'_2+l'}$.
- [20] J. M. Hutson and S. Green, MOLSCAT computer code, version 14 (1994), distributed by Collaborative Computational Project No. 6 of the Engineering and Physical Research Council (UK).
- [21] G. Zarur and H. Rabitz, *J. Chem. Phys.* **60**, 2057 (1974).
- [22] A. Aguado, C. Suárez, and M. Paniagua, *J. Chem. Phys.* **101**, 4004 (1994).
- [23] V. Zeman, University of Toronto (private communication).
- [24] N. Balakrishnan, R.C. Forrey, and A. Dalgarno, *Phys. Rev. Lett.* **80**, 3224 (1998); R.C. Forrey, N. Balakrishnan, A. Dalgarno, M.R. Haggerty, and E.J. Heller, *Phys. Rev. Lett.* **82**, 2657 (1999); E. Bodo, F.A. Gianturco, and A. Dalgarno, *J. Chem. Phys.* **116**, 9222 (2002).
- [25] D.J. Heinzen, R. Wynar, P.D. Drummond, and K.V. Kheruntsyan, *Phys. Rev. Lett.* **84**, 5029 (2000).
- [26] A.V. Avdeenkov and J.L. Bohn, *Phys. Rev. A* **64**, 052703 (2001); J.L. Bohn, *Phys. Rev. A* **62**, 032701 (2000); A. Volpi and J.L. Bohn, *Phys. Rev. A* **65**, 052712 (2002).
- [27] R.N. Zare first suggested applying phase control to ultracold collisions in *Faraday Discuss. Chem. Soc.* **113**, p351 (1999).
- [28] Even in the zero collision energy limit, it is still possible that many partial waves contribute to the cross section, e.g., when the interaction potential approaches zero as $1/R^3$ [6].
- [29] In the close-coupling calculations, it is found that, even though the total cross section has quickly converged, substantially increasing the cut-off value of the total angular momentum may cause some artificial oscillations in the differential cross sections for θ very close to 0 or π .
- [30] D.C. Clary, *Chem. Phys. Lett.* **74**, 454 (1980); R. Hernández, R. Toumi, and D. Clary, *J. Chem. Phys.* **102**, 9544 (1995).
- [31] V.A. Zenevich and G. Billing, *J. Chem. Phys.* **111**, 2401 (1999).
- [32] S. Skokov and J. M. Bowman, *Phys. Chem. Chem. Phys.* **2**, 495 (2000).
- [33] Direct wavepacket propagation is a powerful tool to extract scattering information. Wavepacket propagation would be formally and easily done if the scattering eigenfunction and eigenenergy in the continuum are known. The central idea of the approach in Ref. [32] is to replace the non- L^2 scattering eigenstates by real L^2 states which can be numerically treated. To do this, the continuum is discretized in a box and real eigenstates are obtained. The wavepacket evolution can then be carried out almost trivially. To avoid unphysical reflections at the grid edges, the wavepacket is damped at each time step. In obtaining eigenfunctions, a potential-optimized discrete variable representation is employed, and the truncation/recoupling technique is essential for efficient calculations.
- [34] E. Hagley, X. Maître, G. Noguez, C. Wunderlich, M. Brune, J.M. Raimond, and S. Haroche, *Phys. Rev. Lett.* **79**, 1 (1997); Q.A. Turchette, C.S. Wood, B.E. King, C.J. Myatt, D. Leibfried, W.M. Itano, C. Monroe, and D.J. Wineland, *Phys. Rev. Lett.* **81**, 3631 (1998); B. Julsgaard, A. Kozhekin, and E.S. Polzik, *Nature* **413**, 400 (2001).
- [35] H. Pu and P. Meystre, *Phys. Rev. Lett.* **85**, 3987 (2000); L.-M. Duan, A. Sørensen, J.I. Cirac, and P. Zoller, *Phys. Rev. Lett.* **85**, 3991 (2000).
- [36] K. Bergmann, H. Theuer, and B.W. Shore, *Rev. Mod. Phys.* **70**, 1003 (1998).

- [37] R.G. Unanyan, M. Fleischhauer, K. Bergmann, and B.W. Shore, *Opt. Commun.* **155**, 144 (1998); H. Theuer, R.G. Unanyan, C. Habscheid, K. Klein, and K. Bergmann, *Optics Express* **4**, 77 (1999).